Clinical & Experimental Immunology
The Journal of Translational Immunology

Clinical and Experimental Immunology ORIGINAL ARTICLE doi:10.1111/cei.12452

B7x/B7-H4 modulates the adaptive immune response and ameliorates renal injury in antibody-mediated nephritis

R. D. Pawar,*† B. Goilav,‡ Y. Xia,*† L. Herlitz,§ J. Doerner,† S. Chalmers,† K. Ghosh,† X. Zang† and C. Putterman*†

*The Divisions of Rheumatology, †Department of Microbiology & Immunology, ‡Pediatric Nephrology, Albert Einstein College of Medicine, and §The Department of Pathology, Columbia University Medical Center, NY, USA

Accepted for publication 7 September 2014
Correspondence: C. Putterman, Division of Rheumatology, Albert Einstein College of Medicine, F701N, 1300 Morris Park Avenue, Bronx, NY 10461, USA.
E-mail: chaim.putterman@einstein.yu.edu

Summary

Kidney disease is one of the leading causes of death in patients with lupus and other autoimmune diseases affecting the kidney, and is associated with deposition of antibodies as well as infiltration of T lymphocytes and macrophages, which are responsible for initiation and/or exacerbation of inflammation and tissue injury. Current treatment options have relatively limited efficacy; therefore, novel targets need to be explored. The co-inhibitory molecule, B7x, a new member of the B7 family expressed predominantly by non-lymphoid tissues, has been shown to inhibit the proliferation, activation and functional responses of CD4 and CD8 T cells. In this study, we found that B7x was expressed by intrinsic renal cells, and was up-regulated upon stimulation with inflammatory triggers. After passive administration of antibodies against glomerular antigens, B7x$^{-/-}$ mice developed severe renal injury accompanied by a robust adaptive immune response and kidney up-regulation of inflammatory mediators, as well as local infiltration of T cells and macrophages. Furthermore, macrophages in the spleen of B7x$^{-/-}$ mice were polarized to an inflammatory phenotype. Finally, treatment with B7x-immunoglobulin (Ig) in this nephritis model decreased kidney damage and reduced local inflammation. We propose that B7x can modulate kidney damage in autoimmune diseases including lupus nephritis and anti-glomerular basement membrane disease. Thus, B7x mimetics may be a novel therapeutic option for treatment of immune-mediated kidney disease.

Keywords: B7x, co-inhibition, co-stimulation, nephritis, T cells

Introduction

Activated T cells, in concert with dendritic cells (DC), macrophages and B cells, play a significant role in systemic autoimmunity and in disease pathology [1–4]. For example, kidney involvement in systemic lupus erythmatosus (SLE) (lupus nephritis, LN) is associated with significant infiltration of immune cells and increased levels of inflammatory mediators in the kidneys, which can lead ultimately to severe tissue injury and damage [1–4].

The B7 family of co-stimulatory and co-inhibitory molecules plays an important role in T cell activation or inhibition. Predominant expression of B7 family members is observed in antigen-presenting cells (APC) and in lymphoid tissues. B7-1 (CD80), B7-2 (CD86) and inducible T cell co-stimulator ligand (ICOSL) (B7-h) are co-stimulators of T cell responses, whereas programmed death ligand 1 (PDL1) (B7-H1), PDL2 (B7-DC), B7-H3 and human endogenous retrovirus subfamily H (HERV-H) LTR-associating protein 2 (HHLA2) [5] inhibit T cell proliferation and activation as well as cytokine release [6,7]. T cells express CD28, cytotoxic T lymphocyte antigen-4 (CTLA-4), PD-1 and ICOS which bind to B7 members present on APC, leading to activating or inhibitory signals [6–8].

In order to keep the number of T cells in check and further limit their activation, proliferation, expansion and functional responses, several therapeutic approaches targeting T cell-mediated pathways have been considered for the treatment of diseases involving overactive T cell responses. CTLA-4-immunoglobulin (Ig) is one such approach which is used for patients with LN as well as in rheumatoid arthritis and multiple sclerosis [9–12]. CTLA-4-Ig targets and inhibits the interaction of B7-1 and B7-2 with CD28 on activated T cells. Nevertheless, available treatment options

for blocking co-stimulatory pathways are not effective in many patients; hence, new treatment options need to be explored and evaluated.

B7 family members are expressed by both haematopoietic and non-haematopoietic tissues as well as tumour cells. One new member of the B7 family is B7x (also known as B7-H4, B7S1), which is a negative regulator of T cell proliferation, activation and release of interleukin (IL)-2 and interferon (IFN)-γ [13]. B7x binds to an unknown receptor on T cells which is distinct from CD28, CTLA4, ICOS and PD-1·[6] B7x is expressed predominantly by non-lymphoid (lung, liver, pancreas, testes, ovary, placenta, small intestine, skeletal muscle), rather than lymphoid tissues (spleen and thymus) [7]. B7x is also detectable on activated T cells, B cells, DC, monocytes and macrophages [7]. B7x is the only glycosyl phosphatidylinositol-linked cell membrane protein in the B7 family, and there is 87% amino acid identity between human and mouse B7x [7].

To characterize the role of B7x in immunological disorders, several animal models have been used. B7x was found to restrict immune responses in murine models of autoimmune diabetes, experimental autoimmune encephalitis (EAE) and rheumatoid arthritis [13–20]. However, a possible role in kidney diseases has not been explored previously.

Nephrotoxic serum nephritis is a model of acute kidney injury which is widely used to evaluate mechanisms of kidney injury mediated by pathogenic antibodies, including LN and anti-glomerular basement membrane disease [21–23]. In this model, passively transferred nephrotoxic antibodies deposit in kidneys, activating complement and other inflammatory cascades, which leads to recruitment of immune cells into the kidneys, which further aggravates renal injury [21,22,24–26].

In this study, we found that B7x was expressed by kidney resident cells, and could be induced further with inflammatory stimuli. We further found that B7x$^{-/-}$ mice developed heightened adaptive immune responses and were more susceptible to antibody-mediated nephritis, and exhibited a significant increase in T cell, macrophage and neutrophil infiltration in kidneys compared to the wild-type mice. B7x$^{-/-}$ mice also exhibited polarization of splenic macrophages into an inflammatory M1 phenotype. Therapeutic administration of B7x-Ig in this model attenuated kidney injury and reduced the expression of inflammatory mediators in kidneys, and decreased splenic CD4 and CD8 T cells and inflammatory macrophages. These findings suggest that B7x-Ig or similar mimetics of B7x have potential as a novel treatment option for immune mediated nephritis.

Materials and methods

Mice

Nine to ten 10-week-old C57BL/6 (B6) female mice were purchased from Jackson Laboratories (Bar Harbor, ME, USA). Mice were housed four to five per cage in the animal facility of the Albert Einstein College of Medicine (Bronx, NY, USA) and acclimatized in the facility for 1–2 weeks prior to experiments. B7x$^{-/-}$ mice were bred at the Einstein Institute for Animal Studies. Generation of B7x$^{-/-}$ mice on the B6 background has been described previously [15]. All animal study protocols were approved by the Institutional Animal Care and Use Committee of the Albert Einstein College of Medicine.

Induction of nephrotoxic serum nephritis

Nephrotoxic serum nephritis was induced as described previously [21,22]. Briefly, mouse glomeruli were isolated from female BALB/c mice and sonicated, and this antigenic preparation was used for immunization of rabbits [27]. Rabbit serum collected after sufficient antibody titres were achieved was used as nephrotoxic serum (NTS). Wild-type B6 and B7x$^{-/-}$ mice were primed intraperitoneally (i.p.) with 250 μg of rabbit IgG (Southern Biotech, Birmingham, AL, USA) emulsified with complete Freund's adjuvant (CFA) (Sigma-Aldrich, St Louis, MO, USA) on day 0. On day 5, mice received an intravenous injection of either nephrotoxic serum or phosphate-buffered saline (PBS). Blood and urine were collected at baseline (day 0) and at day 12. Mice were killed on day 12, and kidney tissues were harvested for analysis by histopathology, immunohistochemistry, immunofluorescence and mRNA expression levels. The spleens were obtained for analysis of macrophages, T cells and B cells by flow cytometry.

In-vivo treatment with B7x-Ig

In independent experiments, B6 mice were challenged with NTS as above and treated with B7x-Ig or control Ig (human IgG; BioXcell, West Lebanon, NH, USA) at a dose of 200 μg in 200 μl PBS i.p. per injection on days 6, 9 and 12. An additional control group received the same volume of PBS i.p. following the schedule above. Serum and urine were collected and analysed as above, and the mice were killed at day 12. Kidney tissues were harvested for analysis by histopathology, immunofluorescence and mRNA expression levels, and the spleens were collected for analysis of macrophages, T cells and B cells by flow cytometry.

Enzyme-linked immunosorbent assay (ELISA) for serum IgG

Serum total and class-specific IgG antibodies were measured at day 12. In brief, 96-well microplates were coated with goat anti-mouse IgG, IgG1, IgG2b or IgG3 (Southern Biotech) at 1 μg/ml overnight at 4°C. The plates were washed and blocked with blocking buffer [2% bovine serum albumin (BSA) in PBS], followed by washing and incubation with serum samples or standards for 2 h at

37°C. Alkaline–phosphatase-conjugated anti-mouse IgG or class-specific antibodies (Southern Biotech) were used for the detection of bound antibodies, followed by the addition of phosphatase substrate (Sigma-Aldrich) for colour development, which was read at 405 nm.

Histological analysis

The histology of kidneys from PBS- and NTS-challenged B6 and B7x$^{-/-}$ mice was evaluated by an experienced renal pathologist who was blinded to the mouse strains and treatment groups. Kidney sections were stained with haematoxylin and eosin (H&E) and periodic acid Schiff (PAS), and evaluated for mesangial proliferation, endocapillary proliferation, PAS^{+} deposits and tubulointerstitial lesions, as described previously [21,28]. Between 50 and 100 randomly chosen glomeruli were scored for each mouse. A score from 0 to 4 was given for each parameter above, based on the percentage of glomeruli displaying a particular lesion (0 = not observed, 1 = 1–25%, 2 = 26–50%, 3 = 51–75%, 4 > 75%). Tubulointerstitial lesions, including interstitial inflammation, tubulointerstitial fibrosis, and acute tubular injury were also scored based on the percentage of cortical tissue displaying the pathological lesion, using the 0–4 scale detailed above. Images were captured using light microscopy (Olympus BX41) at ×600 magnification.

Immunohistochemical staining

IgG deposition in kidneys was analysed by immunofluorescence. Kidney sections were deparaffinized by a series of incubations in xylene and decreasing ethanol concentrations (100, 90, 80 and 70%), followed by extensive rinsing with water and PBS. The sections were then blocked separately with biotin and streptavidin blocking reagents (Vector Laboratories, Burlingame, CA, USA) for 15 min each, and washed between each blocking step with Tris-buffered saline containing 0·05% Tween-20 (TBST). Slides were then blocked with PBS containing 2% BSA and 5% normal horse serum (Vector Laboratories) for 30 min, and washed three times. The sections were incubated with biotinylated anti-mouse IgG (Vector Laboratories) for 1 h at room temperature (RT). Sections were washed as above and then incubated with streptavidin-Alexa488 (Jackson ImmunoResearch, West Grove, PA, USA) for 20 min in the dark, and washed again. Slides were covered with mounting medium, and the images captured using fluorescence microscopy (Zeiss Axiscope) at ×400 magnification.

For analysis of neutrophils, T cells and macrophages, the sections were deparaffinized as described above and antigen retrieval was performed using citrate buffer (pH 6) at 95°C for 20 min and washed with distilled water and PBS. The sections were incubated with peroxide block (Dako, Carpinteria, CA, USA), washed three times in TBST and blocked as above. Separate staining with primary antibodies, including rat anti-mouse Ly6G antibody (AbD Serotec, Raleigh, NC, USA), goat anti-human CD3 antibody (eBioscience, San Diego, CA, USA) and rat anti-mouse CD68 antibody (eBioscience), was performed for 2 h at RT. The sections were washed as above and incubated with biotin-conjugated goat anti-rat IgG or goat anti-human IgG for 1 h at RT, followed by streptavidin–horseradish peroxidase (HRP) (Thermo Scientific, Waltham, MA, USA) for 20 min. The 3′,3′-diaminobenzidine (DAB) substrate (Dako) was used for colour development for 1–2 min. Slides were rinsed with water for 5 min, followed by counterstaining with Mayer's haematoxylin (Sigma-Aldrich) for another 2 min. Slides were rinsed in water, air-dried and mounted with Permount (Fisher, Pittsburgh, PA, USA). Images were captured using light microscopy (Zeiss Axiscope) at ×40 magnification.

Real-time polymerase chain reaction (PCR)

RNA was extracted from kidney tissue using the RNeasy minikit (Qiagen, Valencia, CA, USA). For cDNA synthesis, reverse transcription was performed using the SuperScript II system (Invitrogen, San Diego, CA, USA). Real-time PCR was performed in duplicate or triplicate using the SYBR green PCR mastermix (Power SyBr; Applied Biosystems, Warrington, UK) and the ABI PRISM 7900HT Sequence Detection System (Applied Biosystems), and analysed using the $2\wedge\Delta Ct$ method as described previously [22]. Glyceraldehyde 3-phosphate dehydrogenase (GAPDH) was used as a housekeeping gene.

In-vitro stimulation of podocytes, endothelial cells and tubular cells

Podocytes [29], glomerular endothelial cells [30] and tubular cells [31] from established cell lines were used for the stimulation experiments. In brief, cells in Dulbecco's modified Eagle's medium (DMEM) or RPMI-1640 medium (Thermo Scientific) containing 10% fetal bovine serum (FBS) and 1% penicillin and streptomycin (PS) were plated at a density of 10^5/per well in six-well plates. Upon reaching 70% confluence, cells were switched to serum-free media and stimulated with either lipopolysaccharide (LPS) (Invivogen, San Diego, CA, USA) at 5 μg/ml or a combination of tumour necrosis factor (TNF)-α and IFN-γ at 5 ng/ml each (eBioscience) for 6, 12 and 24 h. RNA was isolated using the RNeasy minikit (Qiagen), and real-time PCR for B7x was performed as above. Fold changes in mRNA levels were expressed as a ratio to basal mRNA levels (just prior to stimulation).

For analysis of B7x expression on tubular cells and podocytes by flow cytometry, cells were stimulated for 24 h, harvested and incubated for 10 min in Fc block (anti-mouse CD16/32). Phycoerythrin (PE)-conjugated anti-

mouse B7x antibody (eBioscience) diluted 1:100 in 2% FBS/PBS was added for 30 min, followed by two washes with FBS/PBS. The cells were then analysed by flow cytometry.

Western blot

Podocytes were stimulated for 3, 6 and 12 h, as described above, and the cells harvested using lysis buffer [radioimmunoprecipitation assay (RIPA); Cell Signaling, Danvers, MA, USA] containing a protease inhibitor cocktail (Thermo Scientific). The lysate was centrifuged, and the supernatant was collected and loaded onto a 4–15% TGX gel (Bio-Rad, Hercules, CA, USA) in Tris–glycine–sodium dodecyl sulphate (SDS) buffer for electrophoresis. The transfer was performed using Tris–glycine buffer containing methanol at 4°C for 2 h on a polyvinylidene difluoride (PVDF) membrane (Immobilon, Millipore, Billerica, MA, USA). The membrane was blocked with 5% non-fat dry milk in Tris-buffered saline containing 0·05% Tween-20 (TBST) for 1 h, followed by five washes with TBST. The membrane was incubated overnight with biotin-conjugated goat anti-mouse B7x (R&D Systems, Minneapolis, MN, USA) diluted in blocking buffer at 4°C. The membrane was then washed five times with TBST, incubated with streptavidin–HRP diluted in blocking buffer for 20 min and incubated with enhanced chemiluminescent (ECL) substrate (Pierce, Rockford, IL, USA) for 2–5 min. The density of the bands was calculated using ImageJ software (National Institutes of Health, Bethesda, MD, USA). Relative density was calculated as a ratio to the density of the respective band for β-actin. HRP-conjugated rabbit anti-mouse β-actin antibody (Cell Signaling) was used for detection of β-actin.

Flow cytometry

Splenocytes were prepared from B6 and B7x$^{-/-}$ mice post-challenge, as described previously [32]. In brief, spleens were chopped into fine pieces in ice-cold RPMI-1640 (Invitrogen) medium containing 2% heat-inactivated FBS (Invitrogen) and 1% penicillin–streptomycin (PS), and then passed through 70-μm filters by gentle mincing. The cell suspension was then washed twice with buffer [PBS containing BSA (0·5%) and ethylenediamine tetraacetic acid (EDTA) (0·5 mM)], and treated with a red blood cell (RBC) lysis solution containing 0·14 M NH_4CL, $KHCO_3$ and EDTA, pH7 for 5–10 min at RT. The cells were washed three times with buffer, and incubated with Fc block (anti-mouse CD16/32) for 10 min.

Three staining panels were chosen for separate staining of B cells, T cells and macrophages: (a) CD3, CD4, CD8 and CD25 for T cells; (c) CD19 and MHCII for B cells; and (c) CD11c, CD11b, F480 and Ly6C for macrophages. Antibodies against surface markers were incubated with the cells for 30 min followed by two washes with buffer. The cells were resuspended in buffer, and analysed by flow cytometry using LSRII (BD Biosciences, San Jose, CA, USA) and FlowJo software (Tree Star, Inc., Ashland, OR, USA). A total of 50 000 events were recorded per sample. The antibodies used were PE-CD19, fluorescein isothiocyanate (FITC)-major histocompatibility complex (MHCII), PE-CD3, PE-cyanin (Cy)7-CD4, APC-Cy7-CD8, FITC-CD25, PE-Cy7-CD11c (BD Biosciences), APC-CD11b (Biolegend, San Diego, CA) and peridinin chlorophyll (PerCP-F480) and PE-Ly6C (eBioscience).

Generation of B7x-Ig

A fusion protein of murine B7x and the Fc part of human IgG was constructed as described previously [5,33], followed by expression of the fused protein in Drosophila cells. Cells were grown in Schneider's Drosophila medium (Invitrogen) containing 10% FBS (ultra-low IgG), 1% PS and hygromycin for 7 days, washed with PBS and switched to serum-free media (Express Five; Invitrogen) with 1% PS, hygromycin and 0·05 mM copper sulphate for 7 days for expression of B7x-Ig. The secreted protein was purified from the supernatant using Protein G Hi-trap columns (GE Healthcare, Pittsburgh, PA, USA), dialyzed extensively and sterile-filtered.

Statistical analysis

Differences between groups were compared by a two-tailed unpaired *t*-test unless otherwise indicated. Non-parametric data were analysed using Mann–Whitney's *U*-test. Graphing and statistical analyses were performed using GraphPad Prism (version 4), with *P*-values ≤ 0·05 considered significant.

Results

B7x is up-regulated in renal cells and kidney tissue following inflammatory stimuli

B7x has been reported to be expressed by non-lymphoid organs; therefore, we analysed its expression in several cell types present in kidney, including tubular cells, podocytes and glomerular endothelial cells. We found that all these cell types expressed low levels of B7x mRNA under basal conditions; however, B7x was significantly induced after stimulation in a time-dependent manner (Fig. 1a). In tubular cells, B7x mRNA induction was significant at 6, 12 and 24 h post-stimulation with LPS, whereas with TNF-α + IFN-γ stimulation the increase was significant only at 24 h. In podocytes, the induction of B7x was significant at 6 h post-stimulation with LPS and TNF-α + IFN-γ. In glomerular endothelial cells, significant increases were observed at 6, 12 and 24 h with LPS stimulation, whereas with TNF-α + IFN-γ stimulation the only significant increase was observed at 6 h.

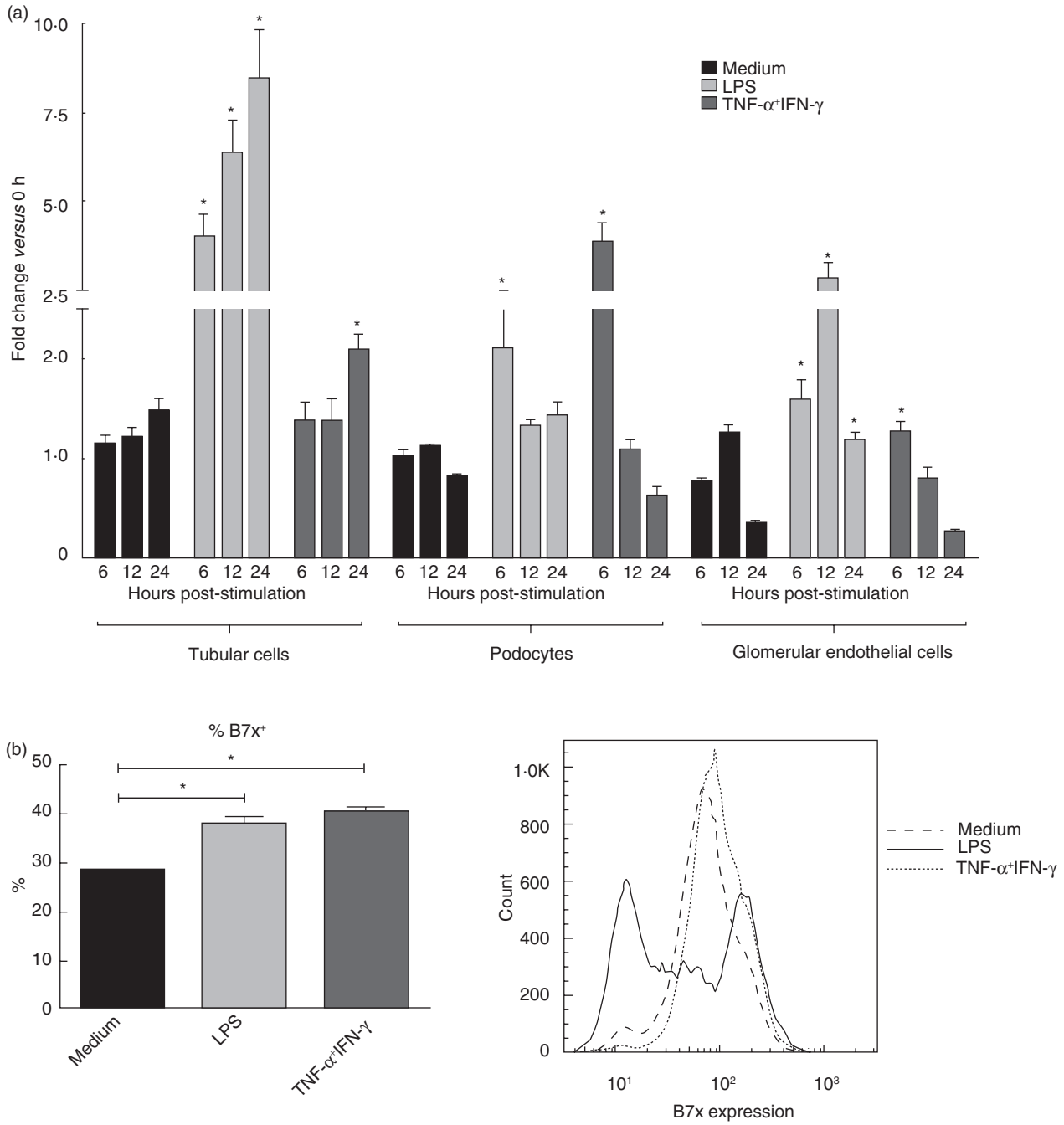

Fig. 1. B7x is up-regulated by inflammatory stimuli. (a) Tubular cells, podocytes and glomerular endothelial cells were stimulated with media alone, lipopolysaccharide (LPS) or tumour necrosis factor (TNF)-α + interferon (IFN)-γ (in triplicate) for 6, 12 and 24 h, and analysed for B7x mRNA levels by real-time polymerase chain reaction (PCR). Fold change in B7x mRNA with each treatment was compared with media alone at each time-point. Data are representative of two independent experiments, and is expressed as mean ± standard error of the mean (s.e.m.). $^*P \leq 0{\cdot}05$, by unpaired *t*-test. (b) Tubular cells were stimulated with media alone, LPS or TNF-α + IFN-γ for 24 h, and B7x expression analysed by flow cytometry. A total of 10 000 events were recorded per sample. Data in the left panel display the mean ± s.e.m. of three independent experiments. $^*P \leq 0{\cdot}05$, by unpaired *t*-test. A representative histogram is shown in the right panel.

To evaluate the protein expression of B7x on resident kidney cells, we performed additional analyses which supported the above findings. Using Western blot, we found that B7x expression in podocytes exists in two different isoforms, 100 kDa and 75 kDa, as described previously in tumours [34], and is up-regulated after stimulation with LPS or TNF-α + IFN-γ (data not shown). Furthermore, using flow cytometry, we found that B7x was induced in

tubular cells post-stimulation with LPS or TNF-α + IFN-γ, confirming the presence of surface B7x on these cells (Fig. 1b). A similar, but much attenuated B7x induction was observed on podocytes but not glomerular endothelial cells following stimulation (data not shown). Endotoxin concentrations in the media were undetectable or negligible (<0·01 EU/ml), and addition of polymyxin B did not alter B7x expression. Furthermore, the effect of LPS on B7x expression was decreased significantly with polymyxin B preincubation, confirming that this effect was specific (data not shown).

B7x deficiency leads to an enhanced humoral immune response

To evaluate the immune response following the NTS challenge, we analysed the levels of total IgG and IgG subclasses in the serum of B6 and B7x$^{-/-}$ mice. Seven days after the serum transfer, B7x$^{-/-}$ mice displayed elevated levels of total IgG ($P = 0{\cdot}02$), IgG2b ($P = 0{\cdot}05$) and IgG1 ($P = 0{\cdot}06$) (Fig. 2a–c) compared to B6 mice. Additionally, levels of anti-rabbit IgG were also found to be significantly higher in B7x$^{-/-}$ mice compared to B6 mice ($P = 0{\cdot}04$) post-NTS challenge (Fig. 2d). Interestingly, basal levels of serum IgG in B7x$^{-/-}$ mice were also higher than the B6 mice ($P = 0{\cdot}01$) (Fig. 2a).

B7x-deficient mice are more susceptible to renal damage and inflammatory cell infiltration

Histological analysis of kidneys revealed that both B6 and B7x$^{-/-}$ mice displayed marked renal damage following passive antibody transfer, with endocapillary hypercellularity, mesangial proliferation, PAS^{+} deposits and tubular lesions (Fig. 2e). However, the most severe indicator of glomerular damage, crescent formation, was more pronounced in B7x$^{-/-}$ mice compared to B6 mice (Fig. 2e). Moreover, the number of infiltrating neutrophils was higher in kidneys of B7x$^{-/-}$ mice compared to B6 mice (Fig. 2f). Kidneys of B6 and B7x$^{-/-}$ mice at baseline (naive) or control challenged with PBS did not show any significant pathology (data not shown).

In nephrotoxic serum nephritis, recruitment and infiltration of immune cells into the kidneys occurs due to the inflammatory cascades initiated after the deposition of antibodies directed against glomerular antigens, followed by up-regulation of inflammatory mediators at the site of injury and complement activation [21,22]. Using immunohistochemical analysis, we found that CD3^{+} T cells and CD68^{+} macrophages were increased significantly in the glomeruli and interstitium of B7x$^{-/-}$ mice compared to B6 mice (Fig. 3a,b). Furthermore, glomerular IgG deposition was more pronounced in B7x$^{-/-}$ mice (Fig. 3c). Finally, B7x was significantly up-regulated in the kidneys of NTS-challenged B6 mice (Fig. 3d). Consistent with the relative overexpression patterns of B7x induced *in vitro* by inflammatory stimuli in resident kidney cells (Fig. 1), *in-vivo* B7x expression was observed primarily in the tubules in this model (Fig. 3d).

Up-regulated levels of inflammatory mediators are found in B7x-deficient kidneys following NTS challenge

Inflammatory cytokines and chemokines as well as other renal injury markers are induced in the kidney post-NTS challenge [21,22]. Therefore, we analysed the levels of inflammatory mediators in the kidney relevant to this model, pre- and post-NTS challenge. When normalized separately to the baseline levels in each strain, we found that levels of CXCL13 ($P < 0{\cdot}05$), IL-23 ($P < 0{\cdot}0001$), IFN regulatory factor 5 (IRF5) ($P < 0{\cdot}01$) and ICOSL ($P < 0{\cdot}01$) were up-regulated markedly in B7x$^{-/-}$ mice compared to B6 mice following induction of nephritis (Fig. 3e). CCL2, CXCL2, CCR5 and TGF-β (Fig. 3e), as well as ICAM-1, regulated upon activation normal T cell expressed and secreted (RANTES) and the pro-apoptotic genes BCL-like protein 4 (BAX) and apoptotic protease activating factor 1 (APAF-1) were at similar levels in both strains post-challenge (data not shown).

Inflammatory macrophages are increased in B7x$^{-/-}$ mice

Splenic macrophages which express CD11b and CD11c can be separated into two subsets (CD11b^{+}CD11c$_{hi}$ or CD11b+CD11c$_{low}$), which can be subdivided further based on the levels of F480 (F480$_{hi}$ or F480$_{low}$) and Ly6C (Ly6c$_{hi}$ or Ly6c$_{low}$) expression. At baseline, there were no differences in any macrophage subset between B6 and B7x$^{-/-}$ mice (data not shown). Analysis of macrophages subpopulations post-NTS challenge revealed that the B7x$^{-/-}$ mice displayed higher relative (%; Fig. 4a) and absolute (9517 ± 616 *versus* 7148 ± 706, $P < 0{\cdot}05$) levels of macrophages which express low levels of

Fig. 2. B7x$^{-/-}$ mice develop a robust humoral immune response, pronounced renal pathology and neutrophil infiltration post-nephrotoxic serum (NTS) challenge. (a–d) Immunoglobulin (Ig)G, IgG2b, IgG1 and anti-rabbit IgG levels in serum of B6 and B7x$^{-/-}$ mice pre- (day 0) and post-challenge (day 12) with NTS. Data are representative of two independent experiments, and are expressed as mean ± standard error of the mean (s.e.m.), $n = 9$–10 per group. *$P \leq 0{\cdot}05$, by unpaired *t*-test. (e) Kidney histopathology was analysed by periodic acid Schiff (PAS) and haematoxylin and eosin (H&E) staining, and images captured at ×600 magnification. A representative image from each strain is shown. Data are expressed as mean ± s.e.m., $n = 9$–10 per group. *$P \leq 0{\cdot}05$, by Mann–Whitney *U*-test. (f) Immunohistochemical analysis of infiltration of Ly6G^{+} neutrophils. Data are expressed as mean ± s.e.m., $n = 6$–7 randomly selected mice per group. *$P \leq 0{\cdot}05$, by Mann–Whitney *U*-test.

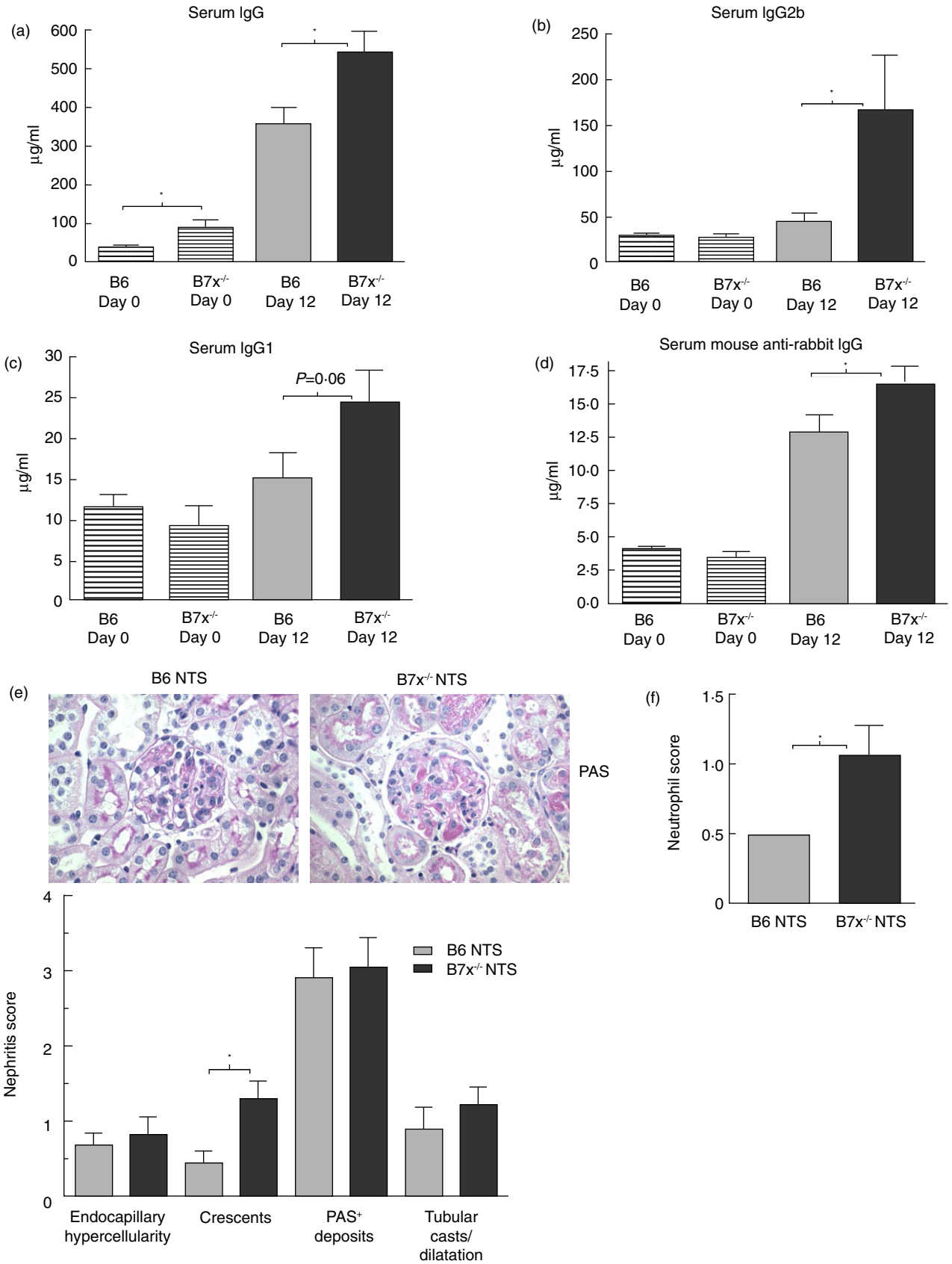
(a)
Serum IgG
µg/ml
600
500
400
300
200
100
0
B6 Day 0
B7x-/- Day 0
B6 Day 12
B7x-/- Day 12
(b)
Serum IgG2b
µg/ml
250
200
150
100
50
0
B6 Day 0
B7x-/- Day 0
B6 Day 12
B7x-/- Day 12
(c)
Serum IgG1
P=0·06
µg/ml
30
25
20
15
10
5
0
B6 Day 0
B7x-/- Day 0
B6 Day 12
B7x-/- Day 12
(d)
Serum mouse anti-rabbit IgG
µg/ml
17·5
15·0
12·5
10·0
7·5
5·0
2·5
0·0
B6 Day 0
B7x-/- Day 0
B6 Day 12
B7x-/- Day 12
(e)
B6 NTS
B7x-/- NTS
PAS
Nephritis score
4
3
2
1
0
B6 NTS
B7x-/- NTS
Endocapillary hypercellularity
Crescents
PAS+ deposits
Tubular casts/ dilatation
(f)
Neutrophil score
1·5
1·0
0·5
0
B6 NTS
B7x-/- NTS

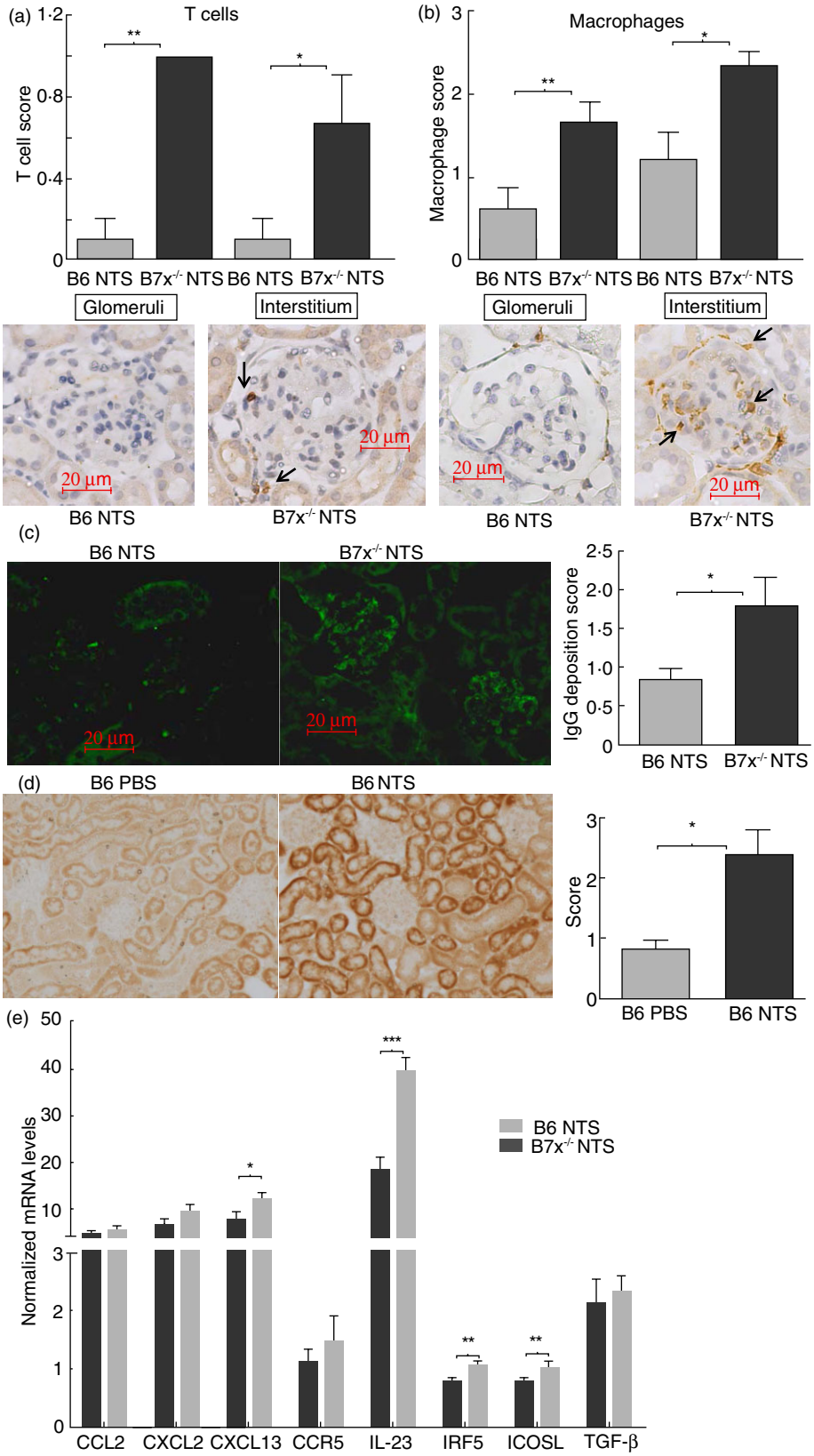

Fig. 3. Exacerbated infiltration of immune cells, immunoglobulin (Ig)G deposition and inflammatory mediator expression in kidneys of B7x$^{-/-}$ mice post-nephrotoxic serum (NTS). (a,b) Immunohistochemical analysis of infiltrating CD3$^+$ T cells and CD68$^+$ macrophages in kidneys of B6 and B7x$^{-/-}$ mice. Data are expressed as mean ± standard error of the mean (s.e.m.), $n = 9$–10 per group. *$P \leq 0{\cdot}05$, by Mann–Whitney *U*-test. Arrows point to positively stained cells in each panel. (c) IgG deposition analysed by immunofluorescence in kidneys of B6 and B7x$^{-/-}$ mice, with images captured at ×400 magnification. Data are expressed as mean ± s.e.m., $n = 6$–7 randomly selected mice per group. *$P \leq 0{\cdot}05$, by Mann–Whitney *U*-test. (d) Immunohistochemical analysis of B7x expression in kidneys of phosphate-buffered saline (PBS) and NTS-challenged B6 mice, with images captured at ×200 magnification. Data are expressed as mean ± s.e.m., $n = 8$ in the PBS and $n = 11$ in the NTS group. *$P \leq 0{\cdot}05$, by Mann–Whitney *U*-test. (e) mRNA expression levels of inflammatory mediators in kidneys of B6 and B7x$^{-/-}$ mice post-NTS challenge, as analysed by real-time polymerase chain reaction (PCR). The relative expression of each mRNA *versus* glyceraldehyde 3-phosphate dehydrogenase (GAPDH) was calculated and normalized with regard to the baseline level of expression in each strain, with the *y*-axis scale × 10^{-3}. Data are representative of two independent experiments, and are expressed as mean ± s.e.m., $n = 9$–10 per group. *$P \leq 0{\cdot}05$, ** $\leq 0{\cdot}01$ and *** $\leq 0{\cdot}001$ by unpaired *t*-test.

F480 (CD11b$^+$CD11c$_{low}$F480$_{low}$) compared to B6 mice. Similarly, there was both a relative (Fig. 4b) and absolute (8989 ± 618 *versus* 6697 ± 706, $P = 0{\cdot}05$) increase in inflammatory type M1 macrophages expressing high levels of Ly6C (CD11b$^+$CD11c$_{low}$F480$_{low}$Ly6c$_{hi}$) in B7x$^{-/-}$ mice. Other macrophage subpopulations (CD11b$^+$CD11c$_{hi}$F480$_{low}$Ly6c$_{low}$, CD11b$^+$CD11c$_{hi}$F480$_{hi}$Ly6c$_{low}$, CD11b$^+$CD11c$_{hi}$F480$_{hi}$, CD11b$^+$ CD11c$_{hi}$F480$_{low}$ and CD11b$^+$CD11c$_{hi}$F480$_{low}$Ly6c$_{hi}$) were at similar levels in both strains challenged with NTS (Fig. 4b and data not shown).

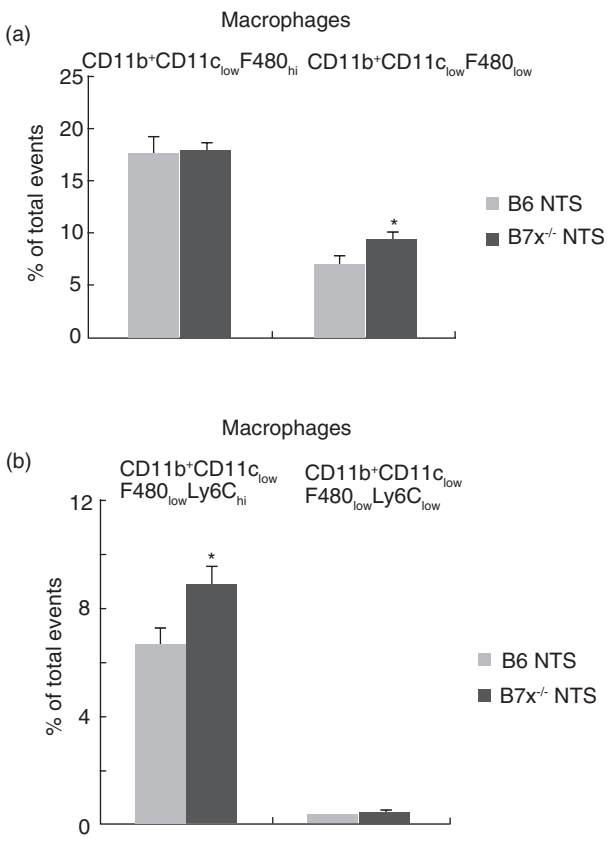

Fig. 4. B7x deficiency modulates macrophage populations in the spleen post-nephrotoxic serum (NTS) challenge. Macrophages were stained as described in the Materials and methods, and a total of 50 000 events were recorded per sample. Data are representative of two independent experiments, and are expressed as mean ± standard error of the mean (s.e.m.), $n = 4$ per group. *$P \leq 0{\cdot}05$, by unpaired *t*-test.

Prechallenge with nephrotoxic sera, there were no significant differences in B or T cell numbers in the spleen between B6 and B7x$^{-/-}$ mice (data not shown). After the exposure, B7x$^{-/-}$ mice displayed a trend towards higher levels of splenic CD4$^+$ and CD8$^+$ T cells as well as activated B cells (CD19$^+$MHCII$^+$) compared to B6 mice (data not shown). Splenic regulatory (CD4$^+$CD25$^+$) T cells were at similar levels in both strains (data not shown).

B7x-Ig attenuates renal damage in NTS-challenged B6 mice

To evaluate the potential of modulation of the B7x pathway as a therapeutic option to restrict immune-mediated damage, we treated NTS-challenged B6 mice with either B7x-Ig or control Ig on days 6, 9 and 12. In contrast to the comparison between the NTS-challenged B7x$^{-/-}$ and B6 mice, the levels of total and class-specific IgG in serum did not show significant differences between the B7x-Ig- and control Ig-treated groups (Fig. 5a–d). However, Ig levels were elevated in both B7x-Ig- and control Ig-treated groups.

NTS challenge induced significant histopathological injury in kidneys of B7x-Ig- and control-treated mice; nevertheless, pathological features in B7x-Ig-treated mice were notably attenuated, especially in terms of endocapillary hypercellularity (Fig. 5e). Furthermore, there was a trend towards fewer PAS$^+$ deposits ($P = 0{\cdot}08$) in B7x-Ig- compared to control Ig-treated mice (Fig. 5e). B7x-Ig-treated mice had significantly decreased kidney T cells in both glomerular ($P = 0{\cdot}01$) and interstitial ($P = 0{\cdot}04$) locations (Fig. 5f). Immunohistochemical analysis of kidney macrophages, infiltrating neutrophils and glomerular IgG deposition showed no significant differences between the groups (data not shown).

B7x-Ig restricts the levels of inflammatory mediators in kidneys

Analysis of inflammatory mediators in kidneys post-NTS challenge revealed that the levels of CXCL2, CXCL13,

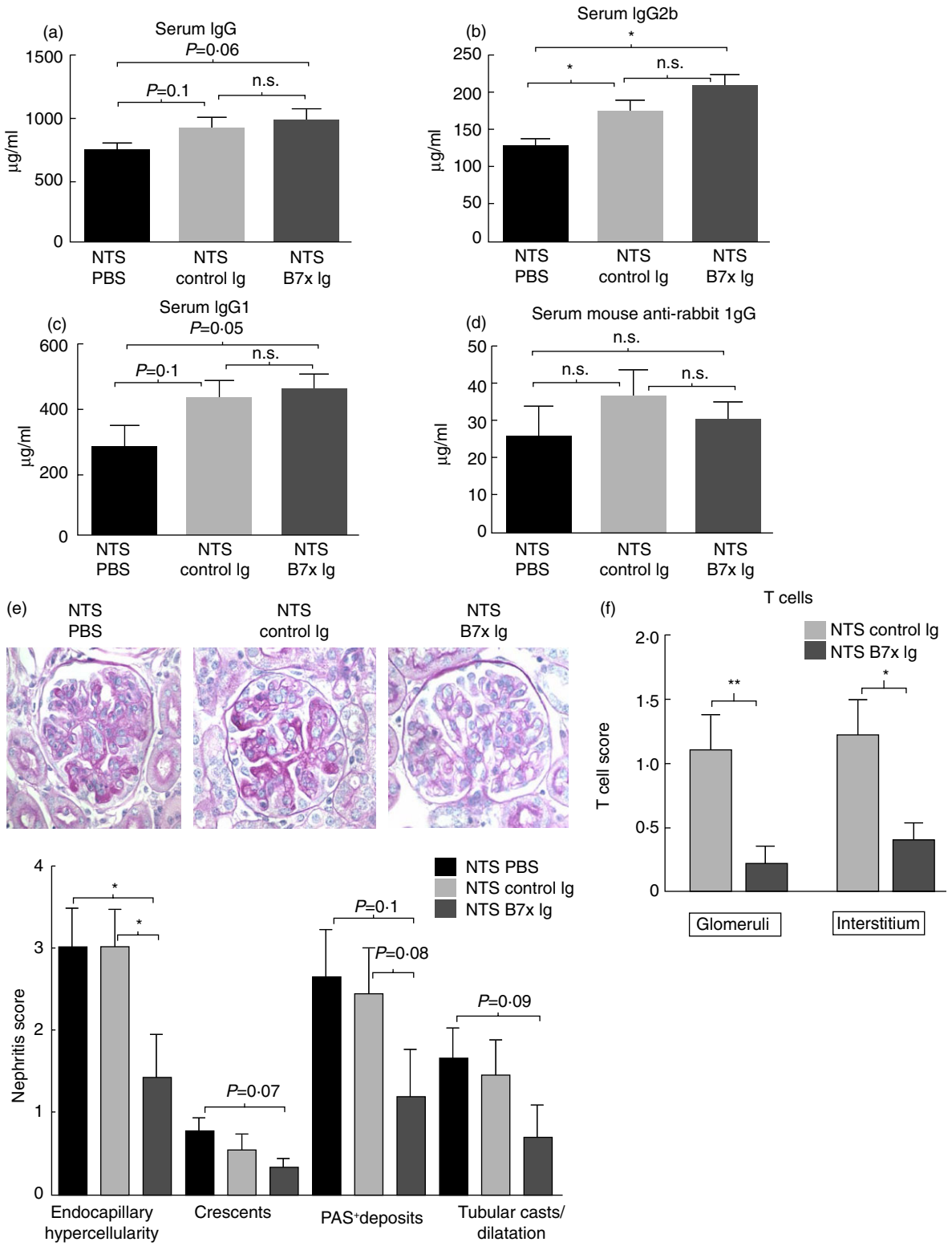

Fig. 5. B7x-immunoglobulin (Ig) treatment restricts renal injury following a nephrotoxic challenge. (a–d) Serum IgG, IgG1, IgG2b, anti-rabbit IgG levels in B7x-Ig, control Ig and phosphate-buffered saline (PBS)-treated mice post-nephrotoxic serum (NTS) challenge. Data are expressed as mean ± standard error of the mean (s.e.m.), $n = 9$–10 per group. *$P \leq 0{\cdot}05$, by unpaired *t*-test. (e) Kidney histopathology was analysed in periodic acid Schiff (PAS) and haematoxylin and eosin (H&E)-stained sections, $n = 9$–10 per group, with images captured at ×600 magnification. A representative section from each group is shown. (f) Immunohistochemical analysis of T cells in kidneys of B7x-Ig- and control Ig-treated mice post-NTS challenge, $n = 9$–10 per group. Data are expressed as mean ± standard error of the mean (s.e.m.). *$P \leq 0{\cdot}05$, ** $\leq 0{\cdot}01$, by Mann–Whitney *U*-test.

CCR5, IRF5, ICOSL and TGF-β were significantly down-regulated in B7x-Ig-treated mice compared to the control-Ig- and PBS-treated mice (Fig. 6a). The levels of CCL2, IP-10, IL-6, IL-23 and TNF did not show any significant differences between the groups (Fig. 6a and data not shown).

B7x-Ig attenuates the expansion of inflammatory macrophages and T cells

Analysis of macrophage subpopulations in the spleen showed that B7x-Ig limited the relative (Fig. 6b,c) and absolute expansion of the $CD11b^+CD11c_{hi}$ macrophage subset (B7x-Ig 1232 ± 168 *versus* control-treated 1680 ± 107, $P = 0{\cdot}07$), and in particular those expressing low levels of F480 ($CD11b^+CD11c_{hi}F480_{low}$) ($864 \pm 114$) compared to control Ig (1251 ± 88, $P = 0{\cdot}04$)- and PBS (1315 ± 90, $P = 0{\cdot}02$)-treated mice. Further analysis of the $CD11b^+CD11c_{hi}F480_{low}$ subset expressing high levels of Ly6C showed that B7x-Ig treatment reduced the relative (Fig. 6d) and absolute number of these inflammatory macrophages (314 ± 73) compared to the control Ig (498 ± 24, $P = 0{\cdot}05$)- and PBS (536 ± 44, $P = 0{\cdot}04$)-treated groups (Fig. 6d). No differences were observed between control Ig- and PBS-treated mice post-NTS challenge (Fig. 6b–d). In addition, $CD11b^+CD11c_{low}$ macrophages and their subsets were found at similar levels in all three treatment groups (data not shown).

Analysis of splenic T cells revealed that $CD4^+$ and $CD8^+$ cells were decreased significantly in the B7x-Ig-treated group compared to control Ig-treated mice (Fig. 6e). Absolute decreases in the number of $CD4^+$ (B7x-Ig: 3916 ± 107, control Ig: 4690 ± 285, $P = 0{\cdot}04$) and $CD8^+$ T cells (B7x-Ig: 3498 ± 83, control Ig: 4189 ± 188, $P = 0{\cdot}02$) were also seen (data not shown). Similarly, activated B cells ($CD19^+MHCII^+$) were reduced in the B7x-Ig treated group, although this did not reach statistical significance (data not shown). Regulatory T cells ($CD4^+CD25^+$) were similar in both groups of mice (Fig. 6e). Control Ig- and PBS-treated mice displayed similar levels of CD4, CD8, regulatory T cells and activated B cells post-NTS challenge (Fig. 6e and data not shown).

Discussion

B7x is a co-inhibitory molecule belonging to the B7 family and expressed by peripheral tissues, which inhibits the proliferation and activation of CD4 and CD8 T cells. In this study we evaluated the role of B7x in nephrotoxic serum nephritis and found that B7x-deficient mice developed a robust humoral response consistent with a role of B7x in regulating adaptive responses, and were more susceptible to renal damage. Specifically, $B7x^{-/-}$ mice displayed enhanced infiltration of T cells and macrophages and more pronounced up-regulation of inflammatory mediators in kidneys, as well as skewing of splenic macrophages towards a M1 inflammatory phenotype. Furthermore, treatment with B7x-Ig attenuated renal injury. *In vitro*, B7x is up-regulated particularly in tubular cells under inflammatory conditions, expanding our understanding of the mechanisms by which resident kidney cells are involved in the pathogenesis of renal inflammatory injury. The robust immune response in $B7x^{-/-}$ mice, together with the functional role of B7x in intrinsic renal cells, probably contributed to the increased expression of inflammatory mediators, cellular infiltration and glomerular IgG deposition following the nephrotoxic insult.

Tissue infiltration by T cells, macrophages and neutrophils and their contribution to inflammation and damage have been well established in several models of kidney disease, and in particular LN. Analysis of renal biopsies from patients with membranous nephropathy, IgA nephropathy, LN and acute allograft rejection revealed that B7x is expressed by tubular epithelium and was induced in patients with severe tubular lesions [35]. Further studies using co-cultures of tubular cells expressing B7x showed that it inhibits cytokine production (IL-2 and IFN-γ) and proliferation of T cells [32].

Our findings are in agreement with a recent report, wherein macrophages expressing high levels of B7x are able to induce regulatory T cells in lymph nodes and restrict injury in experimental adriamycin-induced nephrosis [36]. In autoimmune diabetes $B7x^{-/-}$ mice developed more severe disease, while B7x over-expression in pancreatic islets abrogated disease induction and inhibited $CD4^+$ T cell-mediated effects. Similarly, in EAE, $B7x^{-/-}$ mice developed worse disease and robust T helper type 1 (Th1) and Th17 responses. Interestingly, in contrast to the salutatory effects of B7x in the autoimmune/inflammatory disease models described above, B7x can have a deleterious effect in response to infection and cancer. B7x-deficient mice were more resistant to infection with *Listeria monocytogenes* [37]. Similarly, B7x deficiency provided resistance against *Streptococcus pneumoniae* pulmonary infection, and was associated with a decreased bacterial burden, lower levels of inflammatory cytokines in the lungs and an increase in activated CD4 and CD8 T cells [16]. Finally, patients with renal cell carcinomas expressing B7x are at higher risk of death [38], with higher levels of serum B7x correlating with advanced tumour stage [39]. Altogether, the evidence suggests that B7x is required for restricting the damage in autoimmune diseases; however, it is not essential and can actually be detrimental in infection and cancer, where T cell-mediated clearance of infection and cancer cells is required for optimal protection. Therefore, levels of B7x may need to be controlled carefully while using any future treatment strategies targeting this novel pathway.

We propose that the B7x pathway is a novel therapeutic target in the treatment of renal injury mediated by autoantibodies. We found that B7x-Ig attenuated renal disease following a nephrotoxic insult, inhibited the expan-

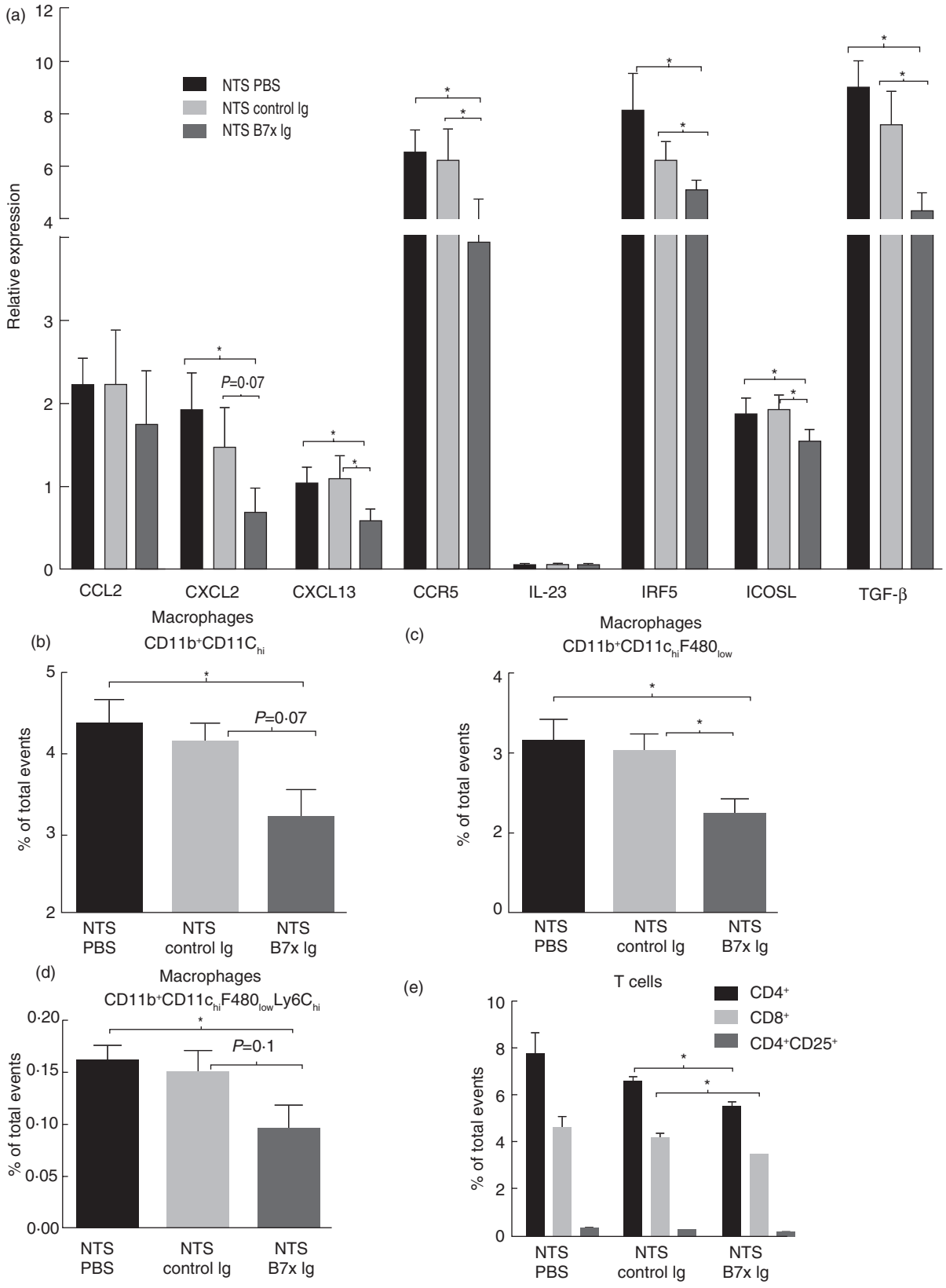
(a)
Relative expression
NTS PBS
NTS control Ig
NTS B7x Ig
P=0·07
CCL2
CXCL2
CXCL13
CCR5
IL-23
IRF5
ICOSL
TGF-β
(b)
Macrophages
CD11b+CD11Chi
% of total events
P=0·07
NTS PBS
NTS control Ig
NTS B7x Ig
(c)
Macrophages
CD11b+CD11chiF480low
% of total events
NTS PBS
NTS control Ig
NTS B7x Ig
(d)
Macrophages
CD11b+CD11chiF480lowLy6Chi
% of total events
P=0·1
NTS PBS
NTS control Ig
NTS B7x Ig
(e)
T cells
CD4+
CD8+
CD4+CD25+
% of total events
NTS PBS
NTS control Ig
NTS B7x Ig

Fig. 6. B7x-immunoglobulin (Ig) treatment attenuates kidney expression of inflammatory mediators and immune cellular infiltrates. (a) mRNA levels of inflammatory mediators in kidneys of B7x-Ig-, control Ig- and phosphate-buffered saline (PBS)-treated mice post-nephrotoxic serum (NTS) challenge. The relative expression of each mRNA *versus* glyceraldehyde 3-phosphate dehydrogenase (GAPDH) is plotted, with the *y*-axis scale $\times 10^{-3}$. Data are expressed as mean ± standard error of the mean (s.e.m.), $n = 9$–10 per group. * $P \leq 0{\cdot}05$, by unpaired *t*-test. (b–d) Macrophages were stained and gated as detailed in the Materials and methods. $CD11b^+CD11c_{hi}$, $CD11b^+CD11c_{hi}F480_{low}$ and $CD11b^+CD11c_{hi}F480_{low}Ly6c_{hi}$ macrophage subpopulations are shown in the figure. A total of 50 000 events were recorded per sample. Data are expressed as mean ± s.e.m., $n = 4$ per group. *$P \leq 0{\cdot}05$, by unpaired *t*-test. (e) $CD4^+$ and $CD8^+$ T cell populations were stained as detailed in the Materials and methods. $CD4^+$ T cells were analysed further for CD25 positivity.

sion of splenic $CD4^+$ and $CD8^+$ T cells and restricted macrophage polarization to an M1 phenotype. M1-type macrophages are believed to be responsible for the aggravation of disease in experimental models of diabetes, renal ischaemia–reperfusion injury and LN [40–44]. B7x-Ig treatment also decreased CXCL13 and IRF5 levels. CXCL13 is associated with the renal damage in human and murine LN [45–48]; IRF5 is a key regulator of the IFN pathway and a genetic risk factor in human SLE [49,50], and plays a prominent role in disease progression in murine lupus [51,52]. In addition, levels of ICOSL, which are associated with the progression of LN [53,54], as well as TGF-β, which is responsible for tubular injury and inflammation [55,56], were decreased by B7x-Ig treatment. Our results are in agreement with other recent studies demonstrating a significant therapeutic benefit of B7x-Ig in autoimmune disease models. B7x-Ig ameliorated progression of EAE and decreased the numbers of activated CD4 T cells in brain and spleen [14], reduced the incidence of autoimmune diabetes in non-obese diabetic (NOD) mice and suppressed islet infiltration by immune cells [17], and modulated CD4 T cell function in inflammatory arthritis, diabetes and allogeneic islet cell transplantation [17–20]. Our findings, together with published studies, indicate collectively that B7x targeted therapies may be a novel strategy for treatment of immune-mediated renal disease, including LN and anti-glomerular basement membrane disease. Nevertheless, the possibility that long-term B7x treatment may increase susceptibility to infectious complications or promote the development of neoplastic disease will certainly need to be investigated carefully.

In summary, we have demonstrated that B7x is expressed in resident kidney cells, and is induced *in vitro* following exposure to inflammatory stimuli and *in vivo* in the context of renal inflammation. Following challenge with nephrotoxic antibodies, B7x-deficient mice develop severe nephritis associated with pronounced kidney T cell and macrophage infiltration. Importantly, therapeutic administration of B7x-Ig restricted histopathological damage, kidney cytokine expression and expansion of splenic M1 macrophages. This study points to a previously unrecognized role of B7x and its receptor in the pathogenesis of renal disease, and suggests that B7x mimetics may have a role as a novel therapeutic option in immune-mediated nephritis.

Acknowledgements

The authors are grateful to the flow cytometry core facility, analytical imaging facility and histopathology facility staff members for scientific advice and technical support. We thank Dr Kimberly Reidy (Albert Einstein College of Medicine) and Dr Alda Tufro (Yale University) for generously providing the glomerular endothelial and podocyte cell lines used for these studies. This study was supported by grants from the NIH RO1-AR048692 and RO1-DK090319 (to C. P.), NIH R01CA175495 and DOD PC131008 (to X. Z.) and an Arthritis Foundation fellowship (#5451) (to R. P.).

Disclosure

None to report.

Author contributions

All authors read the manuscript and had input into revising it for intellectual content and style. For experimental design: R. P., S. C. and C. P.; for acquisition of data: R. P., S. C., J. D., B. G., Y. X. and L. H.; for analysis and interpretation of the data: R. P., S. C., B. G., Y. X., L. H. and C. P. X. Z. and K. G. generated and provided the $B7x^{-/-}$ mice and B7x-Ig producing clone. For drafting of the manuscript: R. P. and C. P.

References

1 Putterman C. New approaches to the renal pathogenicity of anti-DNA antibodies in systemic lupus erythematosus. Autoimmun Rev 2004; **3**:7–11.
2 Kurts C, Panzer U, Anders HJ, Rees AJ. The immune system and kidney disease: basic concepts and clinical implications. Nat Rev Immunol 2013; **13**:738–53.
3 Nowling TK, Gilkeson GS. Mechanisms of tissue injury in lupus nephritis. Arthritis Res Ther 2011; **13**:250.
4 Chan AL, Louie S, Leslie KO, Juarez MM, Albertson TE. Cutting edge issues in Goodpasture's disease. Clin Rev Allergy Immunol 2011; **41**:151–62.
5 Zhao R, Chinai JM, Buhl S *et al*. HHLA2 is a member of the B7 family and inhibits human CD4 and CD8 T-cell function. Proc Natl Acad Sci USA 2013; **110**:9879–84.
6 Zang X, Loke P, Kim J, Murphy K, Waitz R, Allison JP. B7x: a widely expressed B7 family member that inhibits T cell activation. Proc Natl Acad Sci USA 2003; **100**:10388–92.

7 Greenwald RJ, Freeman GJ, Sharpe AH. The B7 family revisited. Annu Rev Immunol 2005; **23**:515–48.

8 Zang X, Allison JP. The B7 family and cancer therapy: costimulation and coinhibition. Clin Cancer Res 2007; **13**:5271–9.

9 Furie R, Nicholls K, Cheng TT *et al*. Efficacy and safety of abatacept in lupus nephritis: a twelve-month, randomized, double-blind study. Arthritis Rheumatol 2014; **66**:379–89.

10 Wofsy D, Hillson JL, Diamond B. Abatacept for lupus nephritis: alternative definitions of complete response support conflicting conclusions. Arthritis Rheum 2012; **64**:3660–5.

11 Genovese MC, Tena CP, Covarrubias A *et al*. Subcutaneous abatacept for the treatment of rheumatoid arthritis: longterm data from the ACQUIRE trial. J Rheumatol 2014; **41**:629–39.

12 Viglietta V, Bourcier K, Buckle GJ *et al*. CTLA4Ig treatment in patients with multiple sclerosis: an open-label, phase 1 clinical trial. Neurology 2008; **71**:917–24.

13 Lee JS, Scandiuzzi L, Ray A *et al*. B7x in the periphery abrogates pancreas-specific damage mediated by self-reactive CD8 T cells. J Immunol 2012; **189**:4165–74.

14 Podojil JR, Liu LN, Marshall SA *et al*. B7-H4Ig inhibits mouse and human T-cell function and treats EAE via IL-10/Treg-dependent mechanisms. J Autoimmun 2013; **44**:71–81.

15 Wei J, Loke P, Zang X, Allison JP. Tissue-specific expression of B7x protects from CD4 T cell-mediated autoimmunity. J Exp Med 2011; **208**:1683–94.

16 Hofmeyer KA, Scandiuzzi L, Ghosh K, Pirofski LA, Zang X. Tissue-expressed B7x affects the immune response to and outcome of lethal pulmonary infection. J Immunol 2012; **189**:3054–63.

17 Wang X, Hao J, Metzger DL *et al*. Early treatment of NOD mice with B7-H4 reduces the incidence of autoimmune diabetes. Diabetes 2011; **60**:3246–55.

18 Wang X, Hao J, Metzger DL *et al*. B7-H4 induces donor-specific tolerance in mouse islet allografts. Cell Transplant 2012; **21**:99–111.

19 Azuma T, Zhu G, Xu H *et al*. Potential role of decoy B7-H4 in the pathogenesis of rheumatoid arthritis: a mouse model informed by clinical data. PLOS Med 2009; **6**:e1000166.

20 Lee IF, Wang X, Hao J *et al*. B7-H4.Ig inhibits the development of type 1 diabetes by regulating Th17 cells in NOD mice. Cell Immunol 2013; **282**:1–8.

21 Xia Y, Campbell SR, Broder A *et al*. Inhibition of the TWEAK/Fn14 pathway attenuates renal disease in nephrotoxic serum nephritis. Clin Immunol 2012; **145**:108–21.

22 Pawar RD, Pitashny M, Gindea S *et al*. Neutrophil gelatinase-associated lipocalin is instrumental in the pathogenesis of antibody-mediated nephritis in mice. Arthritis Rheum 2012; **64**:1620–31.

23 Xia Y, Pawar RD, Nakouzi AS *et al*. The constant region contributes to the antigenic specificity and renal pathogenicity of murine anti-DNA antibodies. J Autoimmun 2012; **39**:398–411.

24 Qing X, Pitashny M, Thomas DB, Barrat FJ, Hogarth MP, Putterman C. Pathogenic anti-DNA antibodies modulate gene expression in mesangial cells: involvement of HMGB1 in anti-DNA antibody-induced renal injury. Immunol Lett 2008; **121**:61–73.

25 Qing X, Zavadil J, Crosby MB *et al*. Nephritogenic anti-DNA antibodies regulate gene expression in MRL/lpr mouse glomerular mesangial cells. Arthritis Rheum 2006; **54**:2198–210.

26 Fujii T, Hamano Y, Ueda S *et al*. Predominant role of FcgammaRIII in the induction of accelerated nephrotoxic glomerulonephritis. Kidney Int 2003; **64**:1406–16.

27 Salant DJ, Cybulsky AV. Experimental glomerulonephritis. Methods Enzymol 1988; **162**:421–61.

28 Herlitz LC, Bomback AS, Markowitz GS *et al*. Pathology after eculizumab in dense deposit disease and C3 GN. J Am Soc Nephrol 2012; **23**:1229–37.

29 Guan F, Villegas G, Teichman J, Mundel P, Tufro A. Autocrine class 3 semaphorin system regulates slit diaphragm proteins and podocyte survival. Kidney Int 2006; **69**:1564–9.

30 Reidy KJ, Villegas G, Teichman J *et al*. Semaphorin3a regulates endothelial cell number and podocyte differentiation during glomerular development. Development 2009; **136**:3979–89.

31 Deocharan B, Qing X, Lichauco J, Putterman C. Alpha-actinin is a cross-reactive renal target for pathogenic anti-DNA antibodies. J Immunol 2002; **168**:3072–8.

32 Pawar RD, Castrezana-Lopez L, Allam R *et al*. Bacterial lipopeptide triggers massive albuminuria in murine lupus nephritis by activating Toll-like receptor 2 at the glomerular filtration barrier. Immunology 2009; **128**:e206–21.

33 Abadi YM, Jeon H, Ohaegbulam KC *et al*. Host b7x promotes pulmonary metastasis of breast cancer. J Immunol 2013; **190**:3806–14.

34 Salceda S, Tang T, Kmet M *et al*. The immunomodulatory protein B7-H4 is overexpressed in breast and ovarian cancers and promotes epithelial cell transformation. Exp Cell Res 2005; **306**:128–41.

35 Chen Y, Yang C, Xie Z *et al*. Expression of the novel co-stimulatory molecule B7-H4 by renal tubular epithelial cells. Kidney Int 2006; **70**:2092–9.

36 Cao Q, Wang Y, Zheng D *et al*. IL-10/TGF-beta-modified macrophages induce regulatory T cells and protect against adriamycin nephrosis. J Am Soc Nephrol 2010; **21**:933–42.

37 Zhu G, Augustine MM, Azuma T *et al*. B7-H4-deficient mice display augmented neutrophil-mediated innate immunity. Blood 2009; **113**:1759–67.

38 Krambeck AE, Thompson RH, Dong H *et al*. B7-H4 expression in renal cell carcinoma and tumor vasculature: associations with cancer progression and survival. Proc Natl Acad Sci USA 2006; **103**:10391–6.

39 Thompson RH, Zang X, Lohse CM *et al*. Serum-soluble B7x is elevated in renal cell carcinoma patients and is associated with advanced stage. Cancer Res 2008; **68**:6054–8.

40 Cucak H, Grunnet LG, Rosendahl A. Accumulation of M1-like macrophages in type 2 diabetic islets is followed by a systemic shift in macrophage polarization. J Leukoc Biol 2014; **95**:149–60.

41 Nieuwenhuizen L, Schutgens RE, Coeleveld K *et al*. Hemarthrosis in hemophilic mice results in alterations in M1-M2 monocyte/macrophage polarization. Thromb Res 2014; **133**:390–5.

42 Bignon A, Gaudin F, Hemon P *et al*. CCR1 inhibition ameliorates the progression of lupus nephritis in NZB/W mice. J Immunol 2014; **192**:886–96.

43 Ranganathan PV, Jayakumar C, Ramesh G. Netrin-1-treated macrophages protect the kidney against ischemia-reperfusion injury and suppress inflammation by inducing M2 polarization. Am J Physiol Renal Physiol 2013; **304**:F948–57.

44 Orme J, Mohan C. Macrophage subpopulations in systemic lupus erythematosus. Discov Med 2012; **13**:151–8.

45 Ezzat M, El-Gammasy T, Shaheen K, Shokr E. Elevated production of serum B-cell-attracting chemokine-1 (BCA-1/CXCL13) is correlated with childhood-onset lupus disease activity, severity, and renal involvement. Lupus 2011; **20**:845–54.
46 Lee HT, Shiao YM, Wu TH *et al*. Serum BLC/CXCL13 concentrations and renal expression of CXCL13/CXCR5 in patients with systemic lupus erythematosus and lupus nephritis. J Rheumatol 2010; **37**:45–52.
47 Schiffer L, Kumpers P, Davalos-Misslitz AM *et al*. B-cell-attracting chemokine CXCL13 as a marker of disease activity and renal involvement in systemic lupus erythematosus (SLE). Nephrol Dial Transplant 2009; **24**:3708–12.
48 Moreth K, Brodbeck R, Babelova A *et al*. The proteoglycan biglycan regulates expression of the B cell chemoattractant CXCL13 and aggravates murine lupus nephritis. J Clin Invest 2010; **120**:4251–72.
49 Niewold TB, Kelly JA, Kariuki SN *et al*. IRF5 haplotypes demonstrate diverse serological associations which predict serum interferon alpha activity and explain the majority of the genetic association with systemic lupus erythematosus. Ann Rheum Dis 2012; **71**:463–8.
50 Cherian TS, Kariuki SN, Franek BS, Buyon JP, Clancy RM, Niewold TB. Brief Report: IRF5 systemic lupus erythematosus risk haplotype is associated with asymptomatic serologic autoimmunity and progression to clinical autoimmunity in mothers of children with neonatal lupus. Arthritis Rheum 2012; **64**:3383–7.
51 Richez C, Yasuda K, Bonegio RG *et al*. IFN regulatory factor 5 is required for disease development in the FcgammaRIIB$^{-/-}$Yaa and FcgammaRIIB$^{-/-}$ mouse models of systemic lupus erythematosus. J Immunol 2010; **184**:796–806.
52 Tada Y, Kondo S, Aoki S *et al*. Interferon regulatory factor 5 is critical for the development of lupus in MRL/lpr mice. Arthritis Rheum 2011; **63**:738–48.
53 Ding H, Wu X, Wu J *et al*. Delivering PD-1 inhibitory signal concomitant with blocking ICOS co-stimulation suppresses lupus-like syndrome in autoimmune BXSB mice. Clin Immunol 2006; **118**:258–67.
54 Iwai H, Abe M, Hirose S *et al*. Involvement of inducible costimulator-B7 homologous protein costimulatory pathway in murine lupus nephritis. J Immunol 2003; **171**:2848–54.
55 Gentle ME, Shi S, Daehn I *et al*. Epithelial cell TGFbeta signaling induces acute tubular injury and interstitial inflammation. J Am Soc Nephrol 2013; **24**:787–99.
56 Iyoda M, Shibata T, Wada Y *et al*. Long- and short-term treatment with imatinib attenuates the development of chronic kidney disease in experimental anti-glomerular basement membrane nephritis. Nephrol Dial Transplant 2013; **28**:576–84.